AIP | The Journal of Chemical Physics

Perspective: Vibrational-induced steric effects in bimolecular reactions

Kopin Liu

Citation: The Journal of Chemical Physics **142**, 080901 (2015); doi: 10.1063/1.4913323
View online: http://dx.doi.org/10.1063/1.4913323
View Table of Contents: http://scitation.aip.org/content/aip/journal/jcp/142/8?ver=pdfcov
Published by the AIP Publishing

Perspective: Vibrational-induced steric effects in bimolecular reactions

Kopin Liu[a)]
Institute of Atomic and Molecular Sciences (IAMS), Academia Sinica, P.O. Box 23-166, Taipei 10617, Taiwan

(Received 19 January 2015; accepted 10 February 2015; published online 23 February 2015)

The concept of preferred collision geometry in a bimolecular reaction is at the heart of reaction dynamics. Exemplified by a series of crossed molecular beam studies on the reactions of a C–H stretch-excited $CHD_3(v_1 = 1)$ with F, Cl, and $O(^3P)$ atoms, two types of steric control of chemical reactivity will be highlighted. A *passive* control is governed in a reaction with strong anisotropic entry valley that can significantly steer the incoming trajectories. This disorientation effect is illustrated by the F and $O(^3P)$ + $CHD_3(v_1 = 1)$ reactions. In the former case, the long-range anisotropic interaction acts like an optical "negative" lens by deflecting the trajectories away from the favored transition-state geometry, and thus inhibiting the bond rupture of the stretch-excited CHD_3. On the contrary, the interaction between $O(^3P)$ and $CHD_3(v_1 = 1)$ behaves as a "positive" lens by funneling the large impact-parameter collisions into the cone of acceptance, and thereby enhances the reactivity. As for reactions with relatively weak anisotropic interactions in the entry valley, an *active* control can be performed by exploiting the polarization property of the infrared excitation laser to polarize the reactants in space, as demonstrated in the reaction of Cl with a pre-aligned $CHD_3(v_1 = 1)$ reactant. A simpler case, the end-on versus side-on collisions, will be elucidated for demonstrating a means to disentangle the impact-parameter averaging. A few general remarks about some closely related issues, such as mode-, bond-selectivity, and Polanyi's rules, are made. © *2015 AIP Publishing LLC.* [http://dx.doi.org/10.1063/1.4913323]

I. INTRODUCTION

It has long been recognized since the early days of reaction dynamics that the nascent product distributions in a chemical reaction are, in general, not in thermal equilibrium.[1] Distilled from numerous infrared (IR) chemiluminescence studies and complementary quasi-classical trajectory (QCT) calculations based on empirically based potential energy surfaces (PES), Polanyi proposed in 1972 a set of rules for qualitatively understanding and predicting the dynamics of atom + diatom reactions.[2,3] The rules concern how the barrier location influences the energy disposal (that is the vibrational and translational distributions of reaction products) and energy requirement (or the capacity of reactant's vibrational and translational energies in promoting the reactivity) in an activated bimolecular reaction. For an exothermic A + BC reaction, the reaction barrier is usually located in the entrance valley of the reaction (an early barrier) by Hammond's postulate.[4] Polanyi's rules then state that reactant translational energy is more efficient than vibration to surmount the barrier, thus, promoting the reaction rate. The converse will be true for an endothermic, late-barrier reaction. Since the energy requirement and the energy disposal are merely the two sides of a coin by microscopic reversibility,[1] the total available energy will be deposited mostly into product vibration for an early-barrier reaction, whereas a translationally hot product will be formed from a late-barrier reaction. Hence, the rule elucidates the role of different forms of energy (vibration versus translation) in an A + BC reaction, and elegantly links its intimate relationship to the location of the barrier. Over the past decades, the rules have stood the test of time and enjoyed great successes.[1]

The situation becomes more complex for polyatomic reactions. The PES has more dimensions, and there are often several transition states leading to different products. More relevantly, there are many more vibrations in the reactant and/or product, and thus different vibrations could exhibit different behaviors. Indeed, one of the central issues in polyatomic reaction dynamics has been the mode-specificity and bond-selectivity. Notably in a series of pioneering studies of the $X + H_2O$ (X = H, Cl)[5–7] and Cl + methane reactions,[8–17] remarkable rate-enhancements by different mode- and/or bond-excitation of reactants were beautifully demonstrated by both the groups of Crim's and Zare's. An intuitively appealing concept emerges and enables a simple means of controlling a chemical reaction, namely, "initial excitation of a motion that has large component along the reaction coordinate should accelerate the reaction."[18] This view also leads to the spectator paradigm that the initial vibrational excitation can largely be retained as the analogous product vibration if the reactant vibrational mode does not couple to the reaction coordinate.[19,20]

While those findings are exciting and intriguing, the implications in the context of Polanyi's rules are ambiguous because the results refer to the same initial collision energy (E_c). To address this issue, Yan *et al.* launched an extensive investigation on the Cl + $CHD_3(v)$ reactions.[21–23] In one of the reports, they measured the relative cross sections of the dominant product channels $HCl(v')$ + $CD_3(0_0)$ for the ground state reactants ($v = 0$), the CH stretch-excited state ($v_1 = 1$), and the bend-excited ($v_b = 1$) CHD_3 over a wide range of E_c.[21] As such, the

a)Email: kliu@po.iams.sinica.edu.tw

relative efficacies of the translation and the vibrational modes can be compared with the equivalent amounts of total initial energy, which is the basis of Polanyi's rules. They found that, in accord with Polanyi's rules, both the stretch- and bend-excitations of CHD_3 are more effective, though not by much, than translation in promoting this late-barrier reaction. [The initial report that "C–H stretch excitation is no more effective than an equivalent amount of translational energy in raising the overall reaction efficiency"[21] was later surpassed when all N-states of $CD_3(0_0)$ were probed—a rotational-probe effect.[24]] Similar findings were found in the analogous Cl + $CH_4(v_3, v_b = 1)$[25–27] and Cl + $CH_2D_2(v_b, v_2$ and $v_6 = 1)$ reactions.[28,29] In those experiments, a single rotational state was selected for the stretch-excited methane. However, Polanyi's rules are originally formulated for a thermal distribution of reactant's rotation,[2,3] for which the effect of reactant rotation is not explicitly accounted for. How to fold the reactant rotational effects on reactivity into the Polanyi's picture remains an interesting subject by itself.

Here, we will address some of the above issues from a radically different perspective—the spatial requirement for chemical reactions. Traditionally, our understanding about chemical reactivity has been focused on the properties of the transition state. In thermal kinetics, barrier height plays a key role, while Polanyi pointed out the importance of barrier location. The stereodynamics, in particular the stereo-requirement, concerns the geometric arrangement of the two reactants, primarily focusing on the saddle point in the literature. As will be elucidated here, two other aspects than the spatial properties of the barrier may also be prominent: the anisotropic part of PES in the entrance valley and the kinematics/dynamics due to the rotational motion of reactants. Three polyatomic reactions will be showcased for this endeavor and for enriching the contents of Polanyi's idea.

Figure 1 depicts schematically the reaction profiles of the three systems. The F + CHD_3 reaction is very exothermic ($\Delta H_{rx} \sim -31.3$ kcal mol^{-1}) with a reactant-like transition state, i.e., an early barrier. The Cl + CHD_3 reaction is slightly endothermic ($\Delta H_{rx} \sim +1.8$ kcal mol^{-1}) and characterized by a product-like transition state or a late barrier. The O(^{3}P) + CHD_3 reaction is also slightly endothermic ($\Delta H_{rx} \sim +2.1$ kcal mol^{-1}). At the transition state, both the O–H and H–C bond lengths are significantly longer than the respective asymptotic lengths, and thus it is neither reactant- nor product-like, i.e., a central barrier. In addition to the diverse barrier locations, the barrier heights of the three reactions are also significantly different. The theoretically calculated adiabatic barriers[30] (the experimentally measured thresholds) are 1.03 kcal mol^{-1} (<0.5 kcal mol^{-1}),[31,32] 3.4 kcal mol^{-1} (~2.5 kcal mol^{-1}),[33,34] and 10.1 kcal mol^{-1} (~8.0 kcal mol^{-1})[35,36] for the ground state reactions of $CHD_3(v = 0)$ with F, Cl, and O(^{3}P), respectively. [The zero-point-energy corrections have been added to the calculated classical barrier heights[30] for the theoretically adiabatic barriers.] In the entrance valley, all three reactions are characterized by two van der Waals (vdW) complexes of C_{3v} symmetry.[30] A deeper well is present as the F (Cl or O(^{3}P)) atom is aligned to the faces of the tetrahedron configuration ($HCH_3 \cdots X$), whereas a shallow well exists at longer distance for the vertex configuration ($H_3CH \cdots X$).

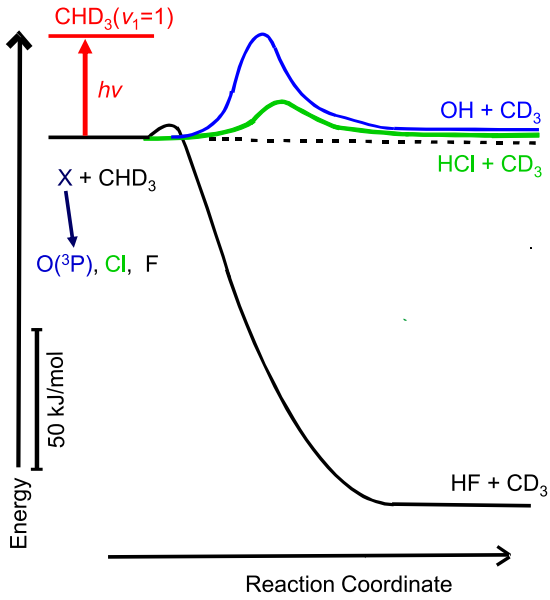

FIG. 1. Schematic representation of the reaction profiles of three H-atom abstraction reactions along the reaction coordinate. All energetic (1 kJ mol^{-1} = 0.239 kcal mol^{-1}) are roughly scaled according to the available experimental results, and the locations of the barriers are in keeping with the *ab initio* calculations. Reproduced with permission from F. Wang and K. Liu, Chem. Sci. **1**, 126-133 (2010). Copyright 2010 by The Royal Society of Chemistry (RSC).

Hence, similar anisotropic topographies, albeit to different extent, are anticipated in the entrance channels of all three ground-state reactions. Upon vibrational excitation, as will be shown later, the anisotropic interactions between the two reactants can alter significantly and result in a remarkable effect on chemical reactivity. We coined this phenomenon the vibrational-induced steric effect. To disentangle the subtle ambiguity from the reactant rotational effect, the same rotational branch of R(1) was used (except for the optical alignment experiment) when preparing the CH stretch-excited $CHD_3(v_1 = 1, j = 2)$ reactants.

II. F + $CHD_3(v_1 = 1)$: AN EARLY BARRIER REACTION

The ground-state reaction has been extensively studied by crossed-beam experiments,[31,32] including the mode correlation between the DF + CHD_2 product pair[37] and the first sighting of reactive resonance in polyatomic reactions.[38–41] Figure 2 shows REMPI (resonance-enhanced multiphoton ionization) spectra of the CHD_2 products from the reaction at $E_c = 3.6$ kcal mol^{-1}.[42] The (2+1) REMPI spectra with the probe laser near 333 nm were recorded in a crossed-beam scattering experiment, and the IR-off and IR-on denote the ground-state and the (IR-induced + residual ground-state) reactions, respectively. The ground-state reaction produces predominantly ground-state $CHD_2(0_0)$ and smaller amounts of vibrationally excited $CHD_2(2_1/3_1/5_1)$ states. With the IR laser on, the intensities of those bands diminished and a new band 1_1^1 appeared, signifying the formation of $CHD_2(v_1 = 1)$ product. Note that the depletion of the dominant $CHD_2(0_0)$ product yields occurs uniformly over the entire REMPI band, indicative of a negligible rotational-probe effect[24]—in contrast to the Cl + CHD_3

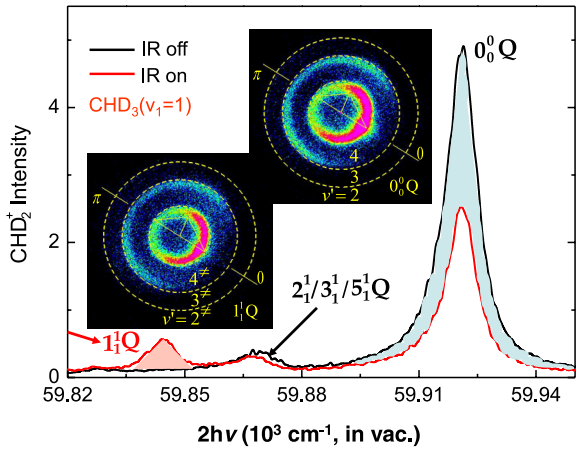

FIG. 2. Two normalized REMPI spectra of the probed CHD_2 products with IR-on (red) and IR-off (black) in the reaction of F + CHD_3 at E_c = 3.6 kcal mol^{-1}. The shaded blue (red) highlights the signal depletion (formation) induced by the IR excitation. Two product images, both with IR-on, are shown for probing of the 1_1^1 Q (left) and 0_0^0 Q (right) bands, respectively. Superimposed on the images are the scattering directions; the 0° angle refers to the initial CHD_3 beam direction in the center-of-mass frame. Reprinted with permission from Zhang *et al.*, Science **325**, 303-306 (2009). Copyright 2009 by AAAS.

case. Also shown in Fig. 2 are the two IR-on images of the probed $CHD_2(v = 0)$ and $CHD_2(v_1 = 1)$ products. The images were recorded by a time-sliced velocity imaging technique,[43] which is capable of revealing quantum-state correlation between the two products—the product pair correlation.[44–46] On energetic ground, the raw images can be easily interpreted by inspection. By conservation of energy and momentum, the maximum velocities of the DF coproducts recoiling from the REMPI-tagged state of CHD_2 were calculated for different final states and depicted as dashed lines in Fig. 2. Energetically, the initial ro-vibrational excitation of $CHD_3(v_1 = 1, j = 2)$ adds 8.63 kcal mol^{-1} to the total energy for the IR-on image, and the formation of $CHD_2(v_1 = 1)$ products requires at least 8.90 kcal mol^{-1}. This near degeneracy results in energetically similar ring radii of the coproduct DF states in the F + $CHD_3(v = 0) \rightarrow CHD_2(v = 0)$ + DF(v') and F + $CHD_3(v_1 = 1) \rightarrow CHD_2(v_1 = 1)$ + DF(v') reactions. Also can be seen, the angular distributions are nearly identical (only subtle differences were noted from detailed image analysis),[42] suggesting similar pathways in the two reactions.

The attenuation of product yields induced by reactant's CH stretch-excitation (Fig. 2) was also observed for other product states, albeit to different extents, including $CHD_2(4_1)$, $CD_3(0_0, 1_1, 2_1, 2_2, 3_1$, and $4_1)$, and a few combination-excited states.[42] From the amounts of the signal depletion for those attenuated CHD_2 and CD_3 states, we estimated their collective production yields in F + $CHD_3(v_1 = 1)$ to be no more than the single product of $CHD_2(v_1 = 1)$. Hence, the CH stretching excitation hinders the overall reaction rate—a totally unexpected finding. For an early barrier reaction, Polanyi's rules would have predicted that a reactant's vibration should not couple efficiently to the reaction coordinate and thus should have little impact on the reaction rate,[2] at variance with the experimental observation of inhibiting the rate. Moreover, although enhanced production of $CHD_2(v_1 = 1)$ in F + $CHD_3(v_1 = 1)$ may be anticipated by the spectator model, one would not expect it to be the only state showing enhancement—a highly mode-specific behavior. The observation of a diminishingly smaller cross section for the H-atom transfer channel upon CH stretching excitation, that is the yields of HF < DF, is another surprise, exemplifying a strong bond selectivity.

It is instructive, albeit rudimentary, to rationalize these surprising results from the viewpoint of the transition state theory. The structure of the transition state of this early barrier reaction is reactant-like, which serves as the bottleneck to reaction. A stretched and compressed C–H bond would result in a deviation from the favored transition-state structures. We then inferred that, upon vibrational excitation, the long-range anisotropic interaction (in the vibrationally adiabatic sense) of F atom with a stretched/compressed C–H must change in a way so that it effectively steers the trajectory away from the transition state, practically shutting down the C–H bond cleavage channel and resulting in a negative impact to total reactivity.[42] The proposed mechanism was shortly confirmed in a QCT calculation,[47,48] based on a full-dimensional *ab initio* PES.[30,49,50] Intuitively, one will expect that this disorientation effect in the entry valley should diminish with increasing collision energy. Indeed, somewhat smaller depletion was reported in a recent study of this reaction at higher collision energy, 9.0 kcal mol^{-1},[51] which is at least ten times larger than the well depths of the vdW complexes. Similar results were also found in the F + $CH_4(v_3 = 1)$[52,53] and F + $CH_2D_2(v_1 = 1$ and $v_6 = 1)$ reactions.[29] Thus, the proposed mechanism appears generally operative for all reactions of CH (symmetrically and/or antisymmetrically) stretch-excited methane with F atom.

III. O(^{3}P) + $CHD_3(v_1 = 1)$: A CENTRAL BARRIER REACTION

In contrast to the F + CHD_3 reaction that is highly exothermic and with a small early barrier, the present reaction is slightly endothermic and with a substantially higher barrier. *Ab initio* calculations indicated that the structure of the transition state is neither reactant- nor product-like, but rather of a "central" barrier.[30,54,55] Again, the ground-state reaction has been extensively investigated and is characterized by a direct abstraction pathway with the rebound mechanism.[35,36,56–63] This is to be contrasted to the ground-state reaction of F + CHD_3, for which dual mechanisms partake: a direct abstraction and a resonance-mediated pathway that prevails at lower collision energies.[38,39]

Figure 3 illustrates the effects of CH stretch-excitation of $CHD_3(v_1 = 1)$ on the $CD_3(v = 0)$ product, which is the dominant product channel.[35] Energetically, the IR-off image shows a single ring-like feature in the backward hemisphere, corresponding to the formation of the OH($v' = 0$) + $CD_3(0_0)$ product pair. The IR-on image exhibits an intense inner ring and a very faint outer ring, and energetically can be ascribed to the OH($v' = 1$) and OH($v' = 0$) coproducts, respectively. Thus, the stretch-excited reaction yields a highly inverted OH vibration distribution in concomitance with the $CD_3(v = 0)$ products. Since the O(^{3}P) + $CHD_3(v_1 = 1)$ reactant channel adiabatically correlates to the OH($v' = 1$) + $CD_3(v = 0)$ product channel,[35] the observed vibrational inversion will imply a predominantly

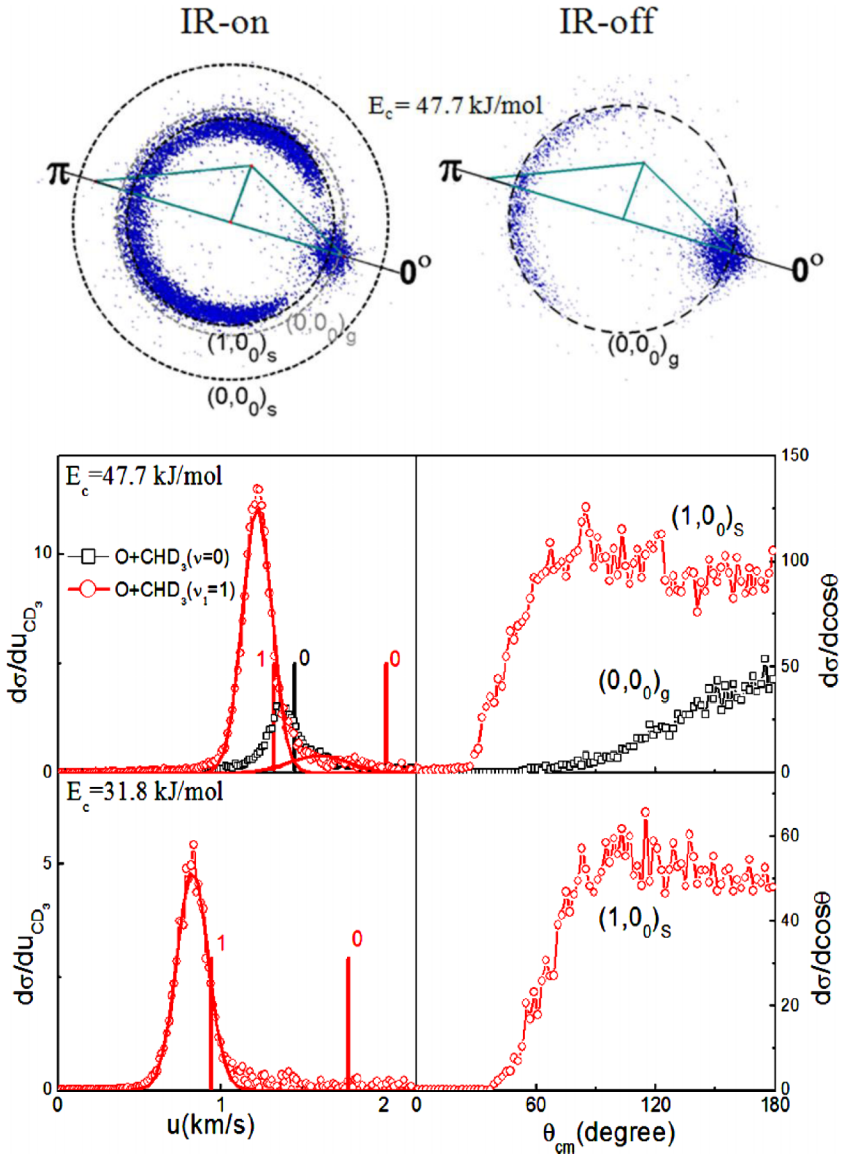

FIG. 3. (Upper) Time-sliced raw images of the probed $CD_3(v=0)$ products from the $O(^3P)+CHD_3$ reaction for IR-on (left) and IR-off (right). Superimposed on the image is the Newton (reactant velocity vectors) diagram. The forward direction, 0°, is defined as the initial CHD_3-beam direction in the center-of-mass frame. The round-shaped feature along 0° is the beam-generated background noise. The ring-like features of the product pairs are assigned as labeled and the dashed circle indicates the maximal recoil speed of the given product pair. The notation of $(1, 0_0)_S$ refers to the (v_{OH}, v_{CD3}) product pair from the stretch-excited reaction ("s"); similarly, the subscript "g" denotes the ground-state reaction. (Lower) The CD_3 product speed distributions (left) and the pair-correlated angular distributions (right) in the ground (in black) and excited states (in red) reactions. The vertical lines mark the CD_3 product speed limits for the concomitantly formed $OH(v=0$ or 1) products. The solid curves are the simulated speed distributions. Reproduced with permission from F. Wang and K. Liu, Chem. Sci. **1**, 126-133 (2010). Copyright 2010 by The Royal Society of Chemistry (RSC).

adiabatic pathway for the H-atom abstraction mechanism. The IR-on image is substantially more intense than the IR-off image (both raw image were experimentally normalized),[35] demonstrating a significant vibrational enhancement in reactivity. The change in product angular distribution, which shifts and extends into the forward hemisphere upon CH stretching excitation, turns out to be more informative. In a direct abstraction reaction, there is a close correlation between the initial impact parameter and the final recoiled direction. We then attributed this change of product angular distribution to the contributions of larger impact-parameter collisions, i.e., enlarging the cone of acceptance.[35] We further surmised that the latter arises from a focusing effect of the long-range anisotropic interactions induced by reactant's stretch-excitation—another manifestation of the vibrational-induced steric effect, yet in complete opposite to the $F + CHD_3$ case. Figure 4 illustrates the contrasting behaviors of the two cases: the anisotropy of the entrance valley in $F + CHD_3(v_1 = 1)$ functions as a negative lens in an optical analogy, whereas that in $O(^3P) + CHD_3(v_1 = 1)$ as a positive lens. A detailed analysis of the opacity function (the reaction probability versus the impact parameter) from QCT and reduced-dimensional quantum dynamics calculations based on a highly accurate *ab initio* PES,[54,57,58] validated experimental conjecture. More recent report on an analogous $O(^3P) + CH_4(v_3 = 1)$ reaction (v_3 is the anti-symmetric stretch mode) also showed a similar effect.[36,62]

The idea that a reactant vibration can open up the cone of acceptance to reaction is not unprecedented. Using a model PES for the $O(^3P) + HCl$ reaction, Schechter and Levine found in a QCT study a new mechanism for vibrationally enhanced reactivity and attributed it to the enlarged reactive cone of acceptance.[64] They also pointed out that such a rate promotion could be particularly prominent for nearly thermo-neutral reaction (as opposed to the late-barrier case for an endothermic reaction) if the symmetric stretch frequency of the transition state is low compared to the vibrational frequency of the reagent. The reaction of $O(^3P) + CHD_3$ clearly fulfills these criteria, both in terms of energetic and the vibrational frequency,[30,54,55] if one treats it as a pseudo A + BC reaction. Recalling the above exothermic $F + CHD_3$ reaction, however, it appears that the vibrational-induced steric effect could be more general than it was originally envisioned.

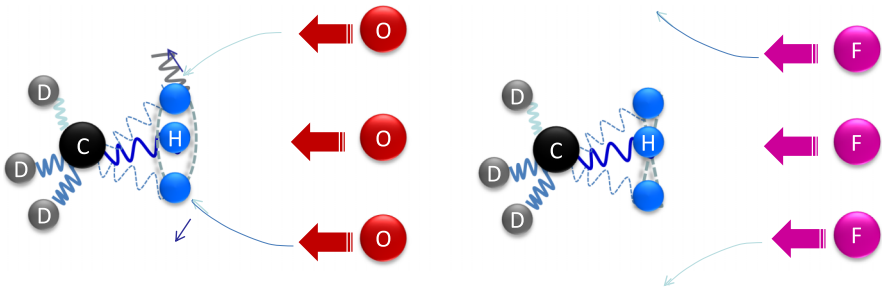

FIG. 4. Cartoon illustrating the vibrational-induced steric effects. The long-range interactions in the reactions of $O(^3P)$ + $CHD_3(v_1 = 1)$ and F + $CHD_3(v_1 = 1)$ exert opposite influences on the trajectories by focusing (defocusing) the $O(^3P)$ atoms (F atoms) into (away) the favored transition state configuration.

In view of the global similarity of the PES landscapes in the vdW region of the ground-state reactions with $O(^3P)$ and F atoms (Sec. I), it is quite remarkable that the same C–H stretching excitation of CHD_3 could result in a completely opposite effect on reactivity: deflecting the trajectory away from the transition state in F + $CHD_3(v_1 = 1)$, while focusing the trajectory into the reactive cone in $O(^3P)$ + $CHD_3(v_1 = 1)$. In an insightful review,[65] Levine introduced the concepts of the physical and chemical shapes of molecules, and how the two shapes influence dynamical stereochemistry. The physical shape of the molecule governs the ability of the reagents to reach the barrier, and thus it is the shape of a molecule as seen by the attacking atom/molecule in the entry valley. The chemical shape refers to the shape near the transition state, i.e., how the barrier height varies with the attack angle or how soft or stiff the bending potential is. Within this framework, both the rate-promotion in $O(^3P)$ + $CHD_3(v_1 = 1)$ and the rate suppression in F + $CHD_3(v_1 = 1)$ are attributed primarily to the different physical shapes of the PES at long range, rather than the transition state properties (the chemical shape). In Levine's language,[65] the same CH stretch-excited $CHD(v_1 = 1)$ reactant will look like an "oblate" when reacting with $O(^3P)$ atom, while as a "prolate" for F atom. One may wonder: Is the change in physical shapes upon reactant's vibrational excitation connected to the barrier location and/or height?

IV. CL + $CHD_3(v_1 = 1)$: A LATE BARRIER REACTION

A. Mechanistic origin of the vibrational enhancement

As the previous $O(^3P)$ + CHD_3 reaction, the present one is also slightly endothermic ($\Delta H_{rx} \sim 1.8$ kcal mol^{-1}). *Ab initio* calculations[30,66,67] suggested a more product-like transition state structure (i.e., a late barrier) with the barrier height of ~3.4 kcal mol^{-1}, in accord with the experimentally measured reaction threshold.[33,34] We note in passing that a late barrier for Cl + CHD_3 and a central barrier for $O(^3P)$ + CHD_3 are not inconsistent with the Hammond's postulate[4] or the Evans-Polanyi model.[1] The postulate or the model states that in a family of related reactions, the more exothermic the reaction is, the earlier the location of the barrier occurs along the reaction coordinate and the more the transition state will resemble the reagents. Hence, the reactions of methane with F, Cl, Br will be in a family, whereas the reaction with $O(^3P)$ will be in a different family with $S(^3P)$ and $Se(^3P)$. As mentioned in Sec. I, this reaction has been the benchmark for studying vibrational effects on reactivity. Many fascinating aspects of mode- and bond-selectivity have been reported, using various deuterated methanes. Here, we shall just focus on one particular aspect: the vibrational enhancement in reaction rate by the stretching excitation of $CHD_3(v_1 = 1)$.

Figure 5 shows the effects of CH stretching excitation in the reaction with Cl atoms.[21] Two raw images shown on the left illustrate the power of the time-sliced velocity-map imaging technique.[43–46] For the IR-off image, several features can be identified and ascribed to the ground-state reaction $(0, 0_0)_g$, the reaction with bend-excited reagents $(0, 0_0)_b$, and the reaction of the spin-orbit excited $Cl(^2P_{1/2})$ atom $(1, 0_0)_{Cl^*}$. That is, with sufficient resolution, all three reactions were simultaneously interrogated. As the IR laser was turned on, a fraction of CHD_3 reagents were ro-vibrationally excited (~20% in this case). Thus, the IR-on image features constitute both the residual IR-off signals (~80% of $(0, 0_0)_g$ and $(1, 0_0)_{Cl^*}$, and 100% of $(0, 0_0)_b$) and new signals from the stretch-excited reaction, as labeled.

Repeating the image measurements over a wide range of collision energies, the resultant excitation functions (the translational energy dependency of the relative cross section) of both the ground-state $(0, 0_0)_g$ and the stretch-excited pairs, $(1, 0_0)_s + (0, 0_0)_s$, are shown in Fig. 5 (right).[21] Clearly, at fixed collision energy (E_c), stretching excitation significantly promotes the reactivity. However, as indicated by the horizontal line, the vibrational enhancement factor in reaction rate appears comparable to the translational factor. As already noted, those experiments were performed at the fixed probe laser wavelength for both convenience and better image resolution, thus only low rotational state of the $CD_3(v = 0)$ products were interrogated.[21] A recent re-investigation,[24] which probed CD_3 ($v = 0$, all $|NK\rangle$ states) by scanning the probe laser wavelength over the entire Q-head of the 0_0^0 band while acquiring the images, showed that the vibrational enhancement factors were actually 2–3 times larger, in accord with the theoretical prediction,[68] as well as Polanyi's rules for this late barrier reaction.

So, the C–H stretching excitation promotes reactivity at fixed collision energies for both $O(^3P)$ + CHD_3 and Cl + CHD_3 reactions. Then, do they have the same mechanistic origin? To unveil that, Figure 6 compares the pair-correlated differential cross sections of the two reactions.[21,35] Despite the difference in collisional energies (both E_c are several kcal mol^{-1} above the respective ground-state reaction thresholds), the behaviors of the stretch-excited reactions are distinct. In the case of Cl + CHD_3,[21] the vibrational enhancement arises from the increase in reaction probability without extending the range of scattering angles, whereas both effects prevail for $O(^3P)$ + CHD_3.[35] In the latter case, we already mentioned that upon CH stretching excitation, the long-range anisotropic

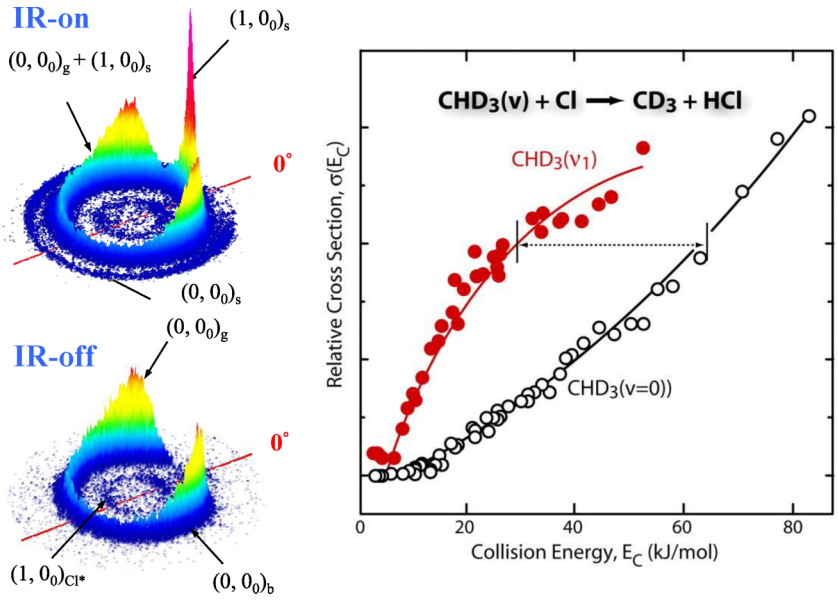

FIG. 5. (Left) Two raw images, IR-on (upper) and IR-off (lower), of the probed $CD_3(v=0$, low $|NK\rangle$ states) products from the Cl + CHD_3 reaction at $E_c = 8.9$ kcal mol^{-1}. The ring-like features in each image are assigned as labeled. (Right) Normalized reactive excitation functions for CH stretch-excited reactant as compared to the ground-state reaction. The solid lines are visual guides. Note the characteristic step feature for a reactive resonance in the stretch-excited reaction near the energetic threshold.[38,39] The horizontal line indicated the equivalent amounts of extra translational energy necessary to achieve reactivity observed upon vibrational excitation. Reprinted with permission from Yan *et al.*, Science **316**, 1723-1726 (2007). Copyright 2007 by AAAS.

interactions will focus the trajectories into the favored reaction geometries, thereby opening up the cone of acceptance and extending the product scattering angles (as indicated by the blue arrow). For Cl + CHD_3, we attributed the increase of reaction probability at a fixed scattered angle (the red arrow) to enlarging the attack angle near the saddle point, i.e., softening the bending potential in the stretch-excited reactions.

Here, the subtle difference of the two concepts is clarified. The "angle of attack" refers to the orientation of the two reacting species at the barrier, i.e., a local stereo-requirement, whereas the "cone of acceptance" also encompasses the steering effects due to the anisotropic interaction en route to the barrier, i.e., a global stereo-requirement. In terms of the angle-dependent line-of-centers model,[1] the reaction cross section can be expressed as

$$\sigma(E_c) = \Pi \iint P(b,\alpha) b db d(\cos\alpha), \qquad (1)$$

where $P(b,\alpha)$ is the opacity function or reaction probability that is a function of both the impact parameter (b) and the angle of attack (α) at the barrier. Roughly speaking, the red arrows in Fig. 6 arise from a broader range of α at a given b and the blue arrow is attributed to the contributions from the larger impact parameter collisions (enlarging the cone of acceptance).

The interpretation that the vibrational rate promotion Cl + $CHD_3(v_1 = 1)$ is mainly governed by a wider attack angle without opening up the reactive cone of acceptance is significant. It implies that the long-range anisotropic interaction in the entrance valley must be relatively weak. In the optical analogy, the interaction will then act like a plane window; no lens-effects. If so, the spatial direction of the reactive C–H bond could be experimentally manipulated by varying the polarization axis of the IR-excitation laser so that the asymptotically prepared reactant approach geometry would largely be retained up to the reaction barrier, which in turn offers the opportunity to probe the dynamical stereochemistry more deeply. Such actively steric-controlled experiments have been performed.[13,69–72] The acquired product images not only unveiled the underlying mechanisms hidden in measurements with unpolarized $CHD_3(v_1 = 1)$ reactants, but also demonstrated unequivocally that both the reaction rate and product distributions can be sterically controlled. With the aid of a theoretical framework,[73] a complete set of the polarization-dependent differential cross section (PDDCSs) of the Cl + $CHD_3(v_1 = 1)$ reaction was also obtained, enabling a clear three-dimensional visualization on how the reaction takes place.[70,72]

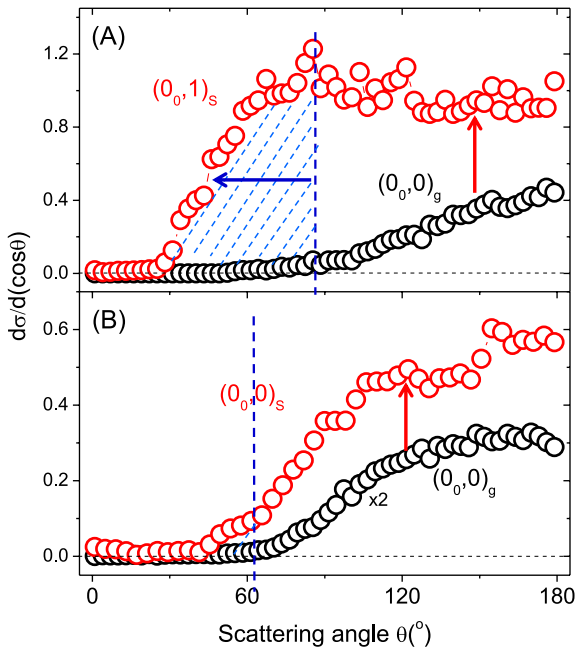

FIG. 6. Comparison of the pair-correlated angular distributions (black for the ground-state and red for the CH stretch-excited reactants) in the (A) O(^{3}P) + CHD_3 and (B) Cl + CHD_3 reactions. Increasing the reaction probability at a fixed scattering angle (the red arrow) is ascribed to the widening of the attack angle near the saddle point. Extending the product scattering angles upon vibrational excitation of reactants (the blue arrow) is attributed to the contributions from larger impact parameter collisions, thus enlarging the cone of the acceptance.

B. Active stereo-control of reactivity

A thorough discussion of a full set of PDDCSs is beyond the scope of this perspective. Here, a less detailed question, yet intuitively more appealing to general chemists, will be addressed: Does the reaction prefer an end-on or a side-on attack?[71] For Cl + $CHD_3(v_1 = 1)$, the two geometries refer to the C–H reactive bond being in parallel (//) or lying in a plane perpendicular (⊥) to the approaching Cl atoms (the $\boldsymbol{k}$-axis), respectively. Since the $v_1 = 1 \leftarrow 0$ vibrational transition is of a parallel band with the transition dipole moment lying along the C–H bond, the two collision geometries can thus be controlled by the polarization direction of a linearly polarized IR laser. When the R(0) transition is exploited to prepare the $CHD_3(v_1 = 1)$ reagents, the resulting probability distribution for the excited C–H bond behaves like a p-orbital aligned with the $\boldsymbol{E}$-field of the IR laser and that of the rotational angular momentum vector for $\boldsymbol{j} = 1$ as a donut for being perpendicular to the C–H bond axis. Hence, experimentally the end-on attack can be achieved by aligning the IR polarization to the $\boldsymbol{k}$-axis, and the side-on approach can be mimicked by directing the IR laser along the $\boldsymbol{k}$-axis and then averaging the results from two orthogonal IR-polarization configurations. As has been shown,[71] the side-on can also be made in a single experimental configuration by setting the $\boldsymbol{E}_{IR}$ direction so that the dihedral angle between the $(\boldsymbol{k}, \boldsymbol{E}_{IR})$ and $(\boldsymbol{k}, \boldsymbol{k}')$ planes is 45°, where $\boldsymbol{k}'$ is the product recoiled velocity.

The upper panels of Figure 7 depict the schematics of the two limiting cases. The lower panels display the corresponding $CD_3(0_0)$ product images from the Cl + $CHD_3(v_1 = 1, |jK\rangle = |10\rangle)$ reaction at $E_c = 3.8$ kcal mol^{-1}. The distinct patterns demonstrated unequivocally a strong alignment effect. The inner ring, corresponding to the $HCl(v' = 1)$ coproducts, features a full circle superimposed with a sharp forward peak that is significantly stronger for the side-on attack. These observations are consistent with the previous assertion that this product channel is likely mediated by a short-lived resonance state.[21,25,29,74] The angular distributions of the outer rings, $HCl(v' = 0)$, are vastly different. While the end-on attack yields predominantly backward-scattered products, the side-on approach clearly gives sideway scatterings. Intuitively, these findings are consistent with a direct abstraction pathway: a rebound type for small impact-parameter collisions and a peripheral type for the larger impact-parameters, though the absence of any backward-scattered products for side-on attack may not be anticipated. Perhaps more significantly, the distinct features of the $HCl(v' = 0)$ images under the two geometries provide a lucid example on how to unfold the impact-parameter averaging by the three vector $(\boldsymbol{k}, \boldsymbol{k}', \boldsymbol{j})$ correlation measurements.[71,75] Since the above two extreme collision geometries exhibit a cylindrical symmetry around the $\boldsymbol{k}$-axis,[71] the conventional integral cross sections can be obtained from the usual image analysis. The results[71] indicated the product state-specific integral cross section (σ) of the $HCl(v' = 0)$ channel favors the end-on attack by a factor of ~1.9, while for $HCl(v' = 1)$ the side-on is preferred by ~1.5. As a result, the branching ratio $\sigma(v' = 0)/\sigma(v' = 1)$ shows a strong dependence on the collision geometry, 3.4 for end-on and 1.2 for side-on. The steric influences on total reactivity, however, are somewhat cancelled by the countered behaviors of the two product channels, about 1.3 times larger for end-on attack.

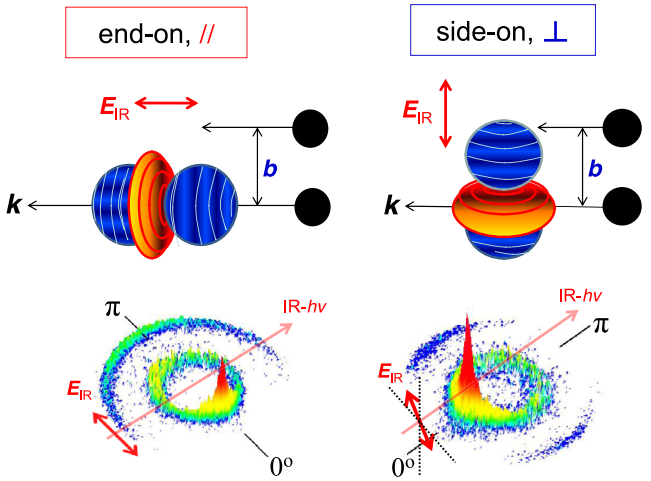

FIG. 7. (Upper) A picturesque representation of the two limiting collision geometries, which can be realized by exploiting the polarization property of the IR excitation laser, $\boldsymbol{E}_{IR}$. The $\boldsymbol{k}$ denoted the initial relative velocity vector and b is the impact parameter. Also depicted in blue (orange) is the probability distribution of the excited C–H bond (the rotational angular momentum $\boldsymbol{j} = 1$) for the IR-excited $CHD_3(v_1 = 1, |jK\rangle = |10\rangle)$ reactants. (Lower) Raw parallel (//, left) and perpendicular (⊥, right) images of the $CD_3(v = 0)$ products from the Cl + prealigned-CHD_3 reaction at $E_c = 3.8$ kcal mol^{-1}. Those are the (IR-on)-(IR-off) difference images. The forward scattering angle 0° denotes the initial CHD_3 beam direction in the center-of-mass frame. In the //-geometry the propagation of IR laser is perpendicular to $\boldsymbol{k}$, and for the ⊥-geometry, the laser direction lies parallel to $\boldsymbol{k}$. The inner ring is assigned to the $HCl(v' = 1)$ products, whereas the outer ring is ascribed to $HCl(v' = 0)$ from the stretch-excited reaction. (The images are reprinted with permission from F. Wang and K. Liu, Chin. J. Chem. Phys. **26**, 705-709 (2013). Copyright 2013 AIP Publishing LLC.)

V. CONCLUDING REMARKS AND OUTLOOK

One of the central concepts for understanding chemical kinetics and reaction dynamics is the steric requirement, which concerns about the preferred collision geometry in a chemical reaction. Traditionally, this requirement is accounted for by the steric A-factor in the Arrhenius rate expression or the angle-dependent barrier height, i.e., the vibrational frequencies transverse to the reaction coordinate at the saddle point, in the transition state theory. As shown here, the steric requirement actually goes beyond the transition state structure (geometry and frequencies): How the trajectories reach the bottleneck to reaction ought also to be considered (a global stereo-requirement). The steering effects exerted by the anisotropic interactions en route to the barrier may result in a positive (as in the $O(^3P)$ + $CHD_3(v_1 = 1)$ reaction) or a negative (as in the F + $CHD_3(v_1 = 1)$ case) impact to chemical reactivity. In those cases, the steric effect is primarily governed by the interaction potential—a passive control. On the other hand, the steric control of a reaction with relatively weak anisotropic potential can be actively performed by polarizing the reactants in the asymptote, as exemplified in the Cl + prealigned $CHD_3(v_1 = 1)$ reaction. In that case, the reaction dynamics will be mainly dictated by the short-range anisotropy of PES, and the measured polarization dependence should provide an incisive probe of the bending potential near the saddle point (the local stereo-requirement).

The three reactions highlighted here, as being prototypical early-, central- and late-barrier reactions, were originally chosen with an intention to generalize Polanyi's rules to polyatomic reactions. Instead, distinct vibrational-induced steric phenomena were unexpectedly uncovered. It is remarkable that three different types of steric effect, or the changes of PES in the entry valley upon vibrational excitation of reactants, are unveiled in the reactions of $O(^3P)$, F, and Cl atoms with the very same $CHD_3(v_1 = 1)$. This succinctly exemplifies the rich dimension of chemistry.

The premise of the vibrational-induced steric effect lies on the concept of vibrational adiabaticity,[1] which should be a reasonably good approximation en route to the barrier, at least for an early or a central barrier reaction. Hence, the change of interactions upon reactant vibration excitation is conceptually embedded in the vibrationally adiabatic PES. In this regard, it is worth noting the sudden vector projection (SVP) model[76,77] proposed by Guo and coworkers for generalizing Polanyi's rules. This is a very significant development in that the SVP model, as well as Polanyi's rules, were tested against the rigorous (or approximate for larger systems) quantum dynamics calculations in a number of benchmark systems, including atom + diatom/polyatomic reactions[76–81] and surface reactions,[82,83] using the available *ab initio* PESs (rather than the empirical London-Eyring-Polanyi-Sato (LEPS) surface). In this sudden limit, the coupling of a reactant mode with the reaction coordinate at the transition state can be approximately quantified by the projection of the former onto the latter—a local stereo-requirement. Thus, the only information needed in the SVP model is the properties of the saddle point, instead of the location of the barrier in the venerable Polanyi's rules. In both cases, the notion that "will the PES in the entry valley help or disrupt the trajectories to reach the barrier?" does not come into the scene. Of course, the sudden and the vibrational-adiabatic dynamics are the two limiting scenarios for physical understanding of chemical reactivity. The adiabatic view would be insightful for reactions with significant anisotropy in the entrance valley and for a deeper understanding of the reactive resonances.[41] On the other hand, the SVP model should work well at sufficiently high translational energy, for which the anisotropy of PES in the entrance channel will have little influence, and for reactions governed by short-range forces (the local stereo-requirement). Obviously, it cannot account for the collisional energy dependency of the reactant mode (vibration vs. translation) preference and the translational propensity almost universally found at lower E_c.[21,25,27,76,77,84,85]

Then, is the vibrational-induced steric effect relevant to Polanyi's rules and the mode-/bond-selectivity? The energy requirement in Polanyi's rules deciphers the relative efficacies of different forms of reactants' energy (vibration or translation) to surmount the reaction barrier. The stereo-requirement concerns the favored transition-state geometry as well as the landscape of PES that the trajectory must travel on its way to the barrier. As mentioned in Sec. I, the general anisotropy in the entrance channel of the three ground-state reactions are alike. Furthermore, *ab initio* calculations of all three reactions[30] showed that the CH stretching frequency decreases substantially en route to the barriers, indicative of significant couplings of this mode to the reaction coordinates. Yet, dramatic changes of the PES topography induced by the very same CH stretching excitation were uncovered. It is tempting to connect the distinct vibrational-induced stereo-specificity to the diverse barrier locations, thus offering an alternative, fresh view of Polanyi's rules. However, it should be pointed out that such apparent correlation will not generally hold for all vibrational modes. Previously, we posited that the activity of a reactant vibrational mode in a reaction will behave as at least one of the three types: spectator, adiabatic, and transitional.[22] In this perspective, we focus only on the effect of the CH stretching mode of excitation, which behave adiabatically in all three reactions. There are many other vibrational modes, 3N-7 left for an N-atom molecule. Depending on the mode-type, different vibrational excitations in a given reaction may exhibit different steric effects and perhaps even change the barrier location from "early" to "late," or vice versa. Since the PES of a chemical reaction is usually anisotropic (either global or local), the suggested vibrational-induced steric effect should be a general phenomenon. As advocated here, one might readily perceive the intimate interconnections among the concepts of the vibrational-induced stereo-specificity, the mode-/bond-selectivity, and Polanyi's rules. Viewing from the big picture, one could even argue that those concepts merely delineate the multifaceted nature of polyatomic reaction dynamics in a different yet complementary way.

The role of reactant rotation is another aspect of stereo-specificity.[65,86,87] Recent experiment[88] and theoretical studies[59,80,89] indicated that the rotational mode of a polyatomic reactant can exert profound and intriguing effects on chemical reactivity. When the reactant is also vibrationally excited, deciphering the (purely) vibrational or the ro-vibrational effects can be a challenging task. For example, on the equivalent amounts of total energy, the CH stretch-excited $CHD_3(v_1 = 1, j = 2)$ promotes the reaction rate with the Cl atom by 2–3 folds.[24] However, over the same collisional energy range of E_c = 2-6 kcal mol^{-1} (compared to the rotational energy of 0.09 kcal mol^{-1} for $j = 2$), a factor of two for the rotational enhancement factor (over the rotationless reactant) of $CHD_3(v_1 = 1, j = 2)$ was found,[88] which nearly accounts for most of the above "vibrational" enhancement factor. Since the reported rate enhancement factor for $CHD_3(v_1 = 1, j = 2)$ was referenced to the reaction with $CHD_3(v = 0, T_{rot} \sim$ 5-10 K), should it be attributed to a pure vibration or a collective ro-vibrational factor? How to incorporate the rotational mode into Polanyi's rules remains an open question.[24] Regardless, all of the above, just to mention a few, will eventually shape our thinking and fundamental understanding of chemical reactivity.

ACKNOWLEDGMENTS

I am indebted to the former and present members of my group at IAMS for their contributions to this decade-long project. This work was financially supported by Academia Sinica and the Minister of Science and Technology of Taiwan (NSC 102-2119-M-001-002-MY3).

[1]R. D. Levine, *Molecular Reaction Dynamics* (Cambridge University Press, Cambridge, 2005).
[2]J. C. Polanyi, Acc. Chem. Res. **5**, 161-168 (1972).

[3]J. C. Polanyi and W. H. Wong, J. Chem. Phys. **51**, 1439-1450 (1969).
[4]G. S. Hammond, J. Am. Chem. Soc. **77**, 334-338 (1955).
[5]A. Sinha, M. C. Hsiao, and F. F. Crim, J. Chem. Phys. **94**, 4928-4935 (1991).
[6]A. Sinha, J. D. Thoemke, and F. F. Crim, J. Chem. Phys. **96**, 372-376 (1992).
[7]M. J. Bronikowski, W. R. Simpson, and R. N. Zare, J. Phys. Chem. **97**, 2194-2203 (1993).
[8]S. Yoon, S. Henton, A. N. Zivkovic, and F. F. Crim, J. Chem. Phys. **116**, 10744-10752 (2002).
[9]S. Yoon, R. J. Holiday, and F. F. Crim, J. Chem. Phys. **119**, 4755-4761 (2003).
[10]S. Yoon, R. J. Holiday, and F. F. Crim, J. Phys. Chem. B **109**, 8388-8392 (2005).
[11]C. J. Annesley, A. E. Berke, and F. F. Crim, J. Phys. Chem. A **112**, 9448-9453 (2008).
[12]S. Yoon, R. J. Holiday, E. L. Sibert III, and F. F. Crim, J. Chem. Phys. **119**, 9568-9575 (2003).
[13]W. R. Simpson, T. P. Rakitzis, S. A. Kandel, A. J. Orr-Ewing, and R. N. Zare, J. Chem. Phys. **103**, 7313-7335 (1995).
[14]H. A. Bechtel, J. P. Camden, D. J. A. Brown, and R. N. Zare, J. Chem. Phys. **120**, 5096-5103 (2004).
[15]H. A. Bechtel, Z. H. Kim, J. P. Camden, and R. N. Zare, J. Chem. Phys. **120**, 791-799 (2004).
[16]H. A. Bechtel, J. P. Camden, D. J. A. Brown, M. R. Martin, R. N. Zare, and K. Vodopyanov, Angew. Chem., Int. Ed. **44**, 2382-2385 (2005).
[17]M. R. Martin, D. J. A. Brown, A. S. Chiou, and R. N. Zare, J. Chem. Phys. **126**, 044315 (2007).
[18]F. F. Crim, Proc. Natl. Acad. Sci. U. S. A. **105**, 12654-12661 (2008).
[19]F. F. Crim, Acc. Chem. Res. **32**, 877-884 (1999).
[20]R. N. Zare, Science **279**, 1875-1879 (1998).
[21]S. Yan, Y.-T. Wu, B. Zhang, X.-F. Yue, and K. Liu, Science **316**, 1723-1726 (2007).
[22]S. Yan, Y.-T. Wu, and K. Liu, Proc. Natl. Acad. Sci. U. S. A. **105**, 12667-12672 (2008).
[23]S. Yan and K. Liu, Chin. J. Chem. Phys. **20**, 333-338 (2007).
[24]F. Wang, J.-S. Lin, Y. Cheng, and K. Liu, J. Phys. Chem. Lett. **4**, 323-327 (2013).
[25]H. Kawamata and K. Liu, J. Chem. Phys. **133**, 124304 (2010).
[26]J. Zhou, J. J. Lin, B. Zhang, and K. Liu, J. Phys. Chem. A **108**, 7832-7836 (2004).
[27]B. Zhang, K. Liu, G. Czako, and J. M. Bowman, Mol. Phys. **110**, 1617-1626 (2012).
[28]Y.-T. Wu and K. Liu, J. Chem. Phys. **129**, 154302 (2008).
[29]J. Riedel, S. Yan, and K. Liu, J. Phys. Chem. A **113**, 14270-14276 (2009).
[30]G. Czako and J. M. Bowman, J. Phys. Chem. A **118**, 2839-2864 (2014).
[31]J. Zhou, J. J. Lin, W. Shiu, S.-C. Pu, and K. Liu, J. Chem. Phys. **119**, 2538-2544 (2003).
[32]W. Shiu, J. J. Lin, K. Liu, M. Wu, and D. H. Parker, J. Chem. Phys. **120**, 117-122 (2004).
[33]J. Zhou, B. Zhang, J. J. Lin, and K. Liu, Mol. Phys. **103**, 1757-1763 (2005).
[34]G. Nyman, J. Zhou, B. Zhang, and K. Liu, Isr. J. Chem. **47**, 1-9 (2007).
[35]F. Wang and K. Liu, Chem. Sci. **1**, 126-133 (2010).
[36]H. Pan and K. Liu, J. Chem. Phys. **140**, 191101 (2014).
[37]J. Zhou, J. J. Lin, and K. Liu, J. Chem. Phys. **119**, 8289-8296 (2003).
[38]J. Zhou, J. J. Lin, and K. Liu, J. Chem. Phys. **121**, 813-818 (2004).
[39]J. Zhou, J. J. Lin, and K. Liu, Mol. Phys. **108**, 957-968 (2010).
[40]K. Liu, J. Chem. Phys. **125**, 132307 (2006).
[41]K. Liu, Adv. Chem. Phys. **149**, 1-46 (2012), and references therein.
[42]W. Zhang, H. Kawamata, and K. Liu, Science **325**, 303-306 (2009).
[43]J. J. Lin, J. Zhou, W. Shiu, and K. Liu, Rev. Sci. Instrum. **74**, 2495-2500 (2003).
[44]J. J. Lin, J. Zhou, W. Shiu, and K. Liu, Science **300**, 966-969 (2003).
[45]J. Zhou, J. J. Lin, W. Shiu, and K. Liu, Phys. Chem. Chem. Phys. **8**, 3000-3006 (2006).
[46]K. Liu, Phys. Chem. Chem. Phys. **9**, 17-30 (2007).
[47]G. Czako and J. M. Bowman, J. Am. Chem. Soc. **131**, 17534-17535 (2009).
[48]G. Czako and J. M. Bowman, J. Chem. Phys. **131**, 244302 (2009).
[49]G. Czako and J. M. Bowman, Phys. Chem. Chem. Phys. **13**, 8306-8312 (2011).
[50]G. Czako, B. C. Shepler, B. J. Braams, and J. M. Bowman, J. Chem. Phys. **130**, 084301 (2009).
[51]J. Yang, D. Zhang, B. Jiang, D. Dai, G. Wu, D. Zhang, and X. Yang, J. Phys. Chem. Lett. **5**, 1790-1794 (2014).
[52]H. Kawamata, W. Zhang, and K. Liu, Faraday Discuss. **157**, 89-100 (2012).
[53]Y. Cheng, H. Pan, F. Wang, and K. Liu, Phys. Chem. Chem. Phys. **16**, 444-452 (2014).
[54]G. Czako and J. M. Bowman, Proc. Natl. Acad. Sci. U. S. A. **109**, 7997-8001 (2012).
[55]E. Gonzalez-Lavado, J. C. Corchado, and J. Espinosa-Garcia, J. Chem. Phys. **140**, 064310 (2014).
[56]R. Liu, M. Yang, G. Czako, J. M. Bowman, J. Li, and H. Guo, J. Phys. Chem. Lett. **3**, 3776-3780 (2012).
[57]G. Czako, R. Liu, M. Yang, J. Bowman, and H. Guo, J. Phys. Chem. A **117**, 6409-6420 (2013).
[58]W. Yan, F. Meng, and D. Wang, J. Phys. Chem. A **117**, 12236-12242 (2013).
[59]G. Czako, J. Phys. Chem. A **118**, 11683-11687 (2014).
[60]G. Czako, J. Chem. Phys. **140**, 231102 (2014).
[61]J. Espinosa-Garica, J. Phys. Chem. A **118**, 3572-3579 (2014).
[62]M. Monge-Palacios, E. Gonzalez-Lavado, and J. Espinosa-Garcia, J. Chem. Phys. **141**, 094307 (2014).
[63]E. Gonzalez-Lavado, C. Rangel, and J. Espinosa-Garcia, Phys. Chem. Chem. Phys. **16**, 8428-8433 (2014).
[64]I. Schechter and R. D. Levine, J. Phys. Chem. **93**, 7973-7975 (1989).
[65]R. D. Levine, J. Phys. Chem. **94**, 8872-8880 (1990).
[66]G. Czako and J. M. Bowman, J. Chem. Phys. **136**, 044307 (2012).
[67]C. Rangel, M. Navarrete, J. C. Corchado, and J. Espinosa-Garcia, J. Chem. Phys. **124**, 124306 (2006).
[68]Z. Zhang, Y. Zhou, D. H. Zhang, G. Czako, and J. M. Bowman, J. Phys. Chem. Lett. **3**, 3416-3419 (2012).
[69]F. Wang, J.-S. Lin, and K. Liu, Science **331**, 900-903 (2011).
[70]F. Wang, K. Liu, and T. P. Rakitzis, Nat. Chem. **4**, 636-641 (2012).
[71]F. Wang and K. Liu, Chin. J. Chem. Phys. **26**, 705-709 (2013).
[72]F. Wang, J.-S. Lin, and K. Liu, J. Chem. Phys. **140**, 084202 (2014).
[73]J. Aldegunde, M. P. de Miranda, J. M. Haigh, B. K. Kendrick, V. Saez-Rabanos, and F. J. Aoiz, J. Phys. Chem. A **109**, 6200-6217 (2005).
[74]B. Zhang and K. Liu, J. Chem. Phys. **122**, 101102 (2005).
[75]D. Herschbach, Eur. Phys. J. D **38**, 3-13 (2006).
[76]H. Guo and B. Jiang, Acc. Chem. Res. **47**, 3679-3685 (2014).
[77]B. Jiang and H. Guo, J. Chin. Chem. Soc. **61**, 847-859 (2014).
[78]B. Jiang and H. Guo, J. Chem. Phys. **138**, 234104 (2013).
[79]J. Li, B. Jiang, and H. Guo, J. Am. Chem. Soc. **135**, 982-985 (2013).
[80]B. Jiang, J. Li, and H. Guo, J. Chem. Phys. **140**, 034112 (2014).
[81]B. Jiang and H. Guo, J. Am. Chem. Soc. **135**, 15251-15256 (2013).
[82]B. Jiang and H. Guo, J. Phys. Chem. C **117**, 16127-16135 (2013).
[83]B. Jiang, R. Liu, J. Li, D. Xie, M. Yang, and H. Guo, Chem. Sci. **4**, 3249-3254 (2013).
[84]G. Czako, Q. Shuai, K. Liu, and J. M. Bowman, J. Chem. Phys. **133**, 131101 (2010).
[85]F. Wang and K. Liu, J. Phys. Chem. A **117**, 8536-8544 (2013).
[86]N. Sathyamurthy, Chem. Rev. **83**, 601-618 (1983), and references therein.
[87]K. Liu, Int. Rev. Phys. Chem. **20**, 189-217 (2001).
[88]R. Liu, F. Wang, B. Jiang, G. Czako, M. Yang, K. Liu, and H. Guo, J. Chem. Phys. **141**, 074310 (2014).
[89]H. Song, J. Li, B. Jiang, M. Yang, Y. Lu, and H. Guo, J. Chem. Phys. **140**, 084307 (2014).